Proc. Natl. Acad. Sci. USA
Vol. 77, No. 8, pp. 4430–4434, August 1980
Biochemistry

Targeting of lipid vesicles: Specificity of carbohydrate receptor analogues for leukocytes in mice

(liposomes/γ-ray perturbed angular correlation spectroscopy/cell surface receptor/drug delivery systems)

MARCIA R. MAUK, RONALD C. GAMBLE, AND JOHN D. BALDESCHWIELER*

Division of Chemistry and Chemical Engineering, California Institute of Technology, Pasadena, California 91125

Contributed by John D. Baldeschwieler, April 7, 1980

ABSTRACT **The presence of particular surface carbohydrate modifications is shown to affect dramatically the stability and tissue specificity of unilamellar distearoyl phosphatidylcholine vesicles in mice. Use of the γ-ray probe $^{111}In^{3+}$ permits analysis of tissue distributions by standard γ counting techniques and determination of the structural integrity of the vesicles by perturbed angular correlation spectroscopy. Addition of a 6-aminomannose derivative of cholesterol to the lipid bilayer produces initial retention of high levels of intact vesicles in the lung after intravenous injection followed by concentration of intact vesicles in the liver and spleen. Vesicles bearing 6-aminosugar residues are found to concentrate in the axillary space in aggregates of polymorphonuclear leukocytes when administered subcutaneously. The *in vivo* stability of 6-aminomannose-labeled vesicles is substantially greater after intravenous or subcutaneous administration than that observed for any other system examined. The dose–response effects observed with surface modifications indicate that a particular receptor topography is important in the mechanism leading to transport and destruction of these vesicles.**

The use of liposomes as carriers for delivery of therapeutic and diagnostic agents to specific targets within the body has been under investigation by a large number of research groups. The complex problems encountered in *in vivo* therapeutic applications (1) clearly suggest the necessity to increase the specificity of liposome targeting. To obtain satisfactory targeting of administered agents, the liposomes must not only reach the appropriate tissue but must also release their contents at the desired time.

Complex carbohydrates are involved in many biological recognition processes including antibody and toxin recognition and cellular adhesion (2). Of particular interest are the findings by Huang (3) and Bussian and Wriston (4) that the interaction of glycolipid-bearing vesicles with cultured cells is carbohydrate specific. This suggests that expansion of our previous studies on *in vivo* vesicle stability (5, 6) may provide insight into the determinants required for recognition by particular tissues. We report here the effects of particular surface carbohydrate modifications on lipid vesicle stability and tissue specificity in mice. These surface modifications are achieved by incorporating carbohydrate derivatives of cholesterol into the lipid bilayer. The use of vesicles containing high levels of $^{111}In^{3+}$ (7) permits analysis of tissue distributions by standard γ counting techniques and determination of the structural integrity of the vesicles by perturbed angular correlation spectroscopy (PAC) (5, 6). Preliminary findings (8) with this approach indicated that vesicles with aminosugar derivatives have the greatest longevity and a specificity for leukocytes.

The publication costs of this article were defrayed in part by page charge payment. This article must therefore be hereby marked "*advertisement*" in accordance with 18 U. S. C. §1734 solely to indicate this fact.

MATERIALS AND METHODS

Materials. L-α-Distearoyl phosphatidylcholine ($Ste_2PtdCho$) from Calbiochem and cholesterol (Chol) from Sigma were used without further purification. Fucosyl, galactosyl, mannosyl, acetamidogalactosyl, aminomannosyl, and aminogalactosyl derivatives of cholesterol (FucChol, GalChol, ManChol, AcAmGalChol, NManChol, and NGalChol, respectively) were gifts from Merck, Sharp & Dohme Research Laboratories (9). The structures of these derivatives of cholesterol are shown in Fig. 1. Dicetyl phosphate (Cet_2P) and stearylamine (NSte) were purchased from Sigma, the trisodium salt of nitrilotriacetic acid [$N(AcOH)_3$] from Aldrich, ultrapure $InCl_3$ from Ventron (Danvers, MA), and heat-inactivated calf serum from GIBCO. Cholesteryl [9,10-^{3}H]oleate (specific activity, 11 Ci/g; 1 Ci = 3.7×10^{10} becquerels) and cholesteryl [1-^{14}C]oleate (51 Ci/mol) were obtained from New England Nuclear. Carrier-free $^{111}InCl_3$ was purchased from Medi+Physics (Glendale, CA) and purified as described (6). The ionophore A23187 was a gift from Eli Lilly.

Preparation of Vesicles. Unilamellar vesicles with A23187 incorporated into the bilayer were prepared as described (5, 7) by probe sonication of lipid mixtures in a buffer solution consisting of 1 mM $N(AcOH)_3$ in 0.9% NaCl/5 mM Na phosphate, pH 7.4. Vesicles of the following compositions (molar ratio) were prepared: $Ste_2PtdCho$/Chol/A23187, 2:1:0.004; $Ste_2PtdCho$/Chol/Cet_2P/A23187, $Ste_2PtdCho$/Chol/NSte/A23187, and $Ste_2PtdCho$/Chol/cholesterol derivative/A23187, all 2:0.5:0.5:0.004. All preparations contained A23187; therefore, reference to it will be omitted hereafter in the designated vesicle compositions. Tritiated (1 μCi) or ^{14}C-labeled cholesteryl oleate (0.5 μCi) were included in the mixtures as a marker for the lipid phase.

After sonication, annealing, and low-speed centrifugation (7, 10), the $N(AcOH)_3$ external to the liposomes was removed by passage of the preparation over a Sephadex G-50 column equilibrated with phosphate-buffered saline. The vesicles were

Abbreviations: PAC, γ-ray perturbed angular correlation; $Ste_2PtdCho$, L-α-distearoyl phosphatidylcholine; Chol, cholesterol; FucChol, GalChol, ManChol, AcAmGalChol, NGalChol, and NManChol, are fucosyl, galactosyl, mannosyl, acetamidogalactosyl, aminogalactosyl, and aminomannosyl derivatives, respectively, of cholesterol [FucChol, 6-(1-thio-1-deoxy-β-L-fucopyranosyl)-1-(cholest-5-en-3β-yloxy)hexane; GalChol, 6-(1-thio-1-deoxy-β-D-galactopyranosyl)-1-(cholest-5-en-3β-yloxy)hexane; ManChol, 6-(5-cholesten-3β-yloxyl)hexyl-1-thio-α-D-mannopyranoside; AcAmGalChol, 6-(5-cholesten-3β-yloxy)hexyl-2-acetamido-2-deoxy-1-thio-β-D-galactopyranoside; NGalChol, 6-(5-cholesten-3β-yloxy)hexyl-6-amino-6-deoxy-1-thio-β-D-galactopyranoside; NManChol, 6-(5-cholesten-3β-yloxy)hexyl-6-amino-6-deoxy-1-thio-α-D-mannopyranoside]; $N(AcOH)_3$, nitrilotriacetic acid; Cet_2P, dicetyl phosphate; NSte, stearylamine.

* To whom reprint requests should be addressed.

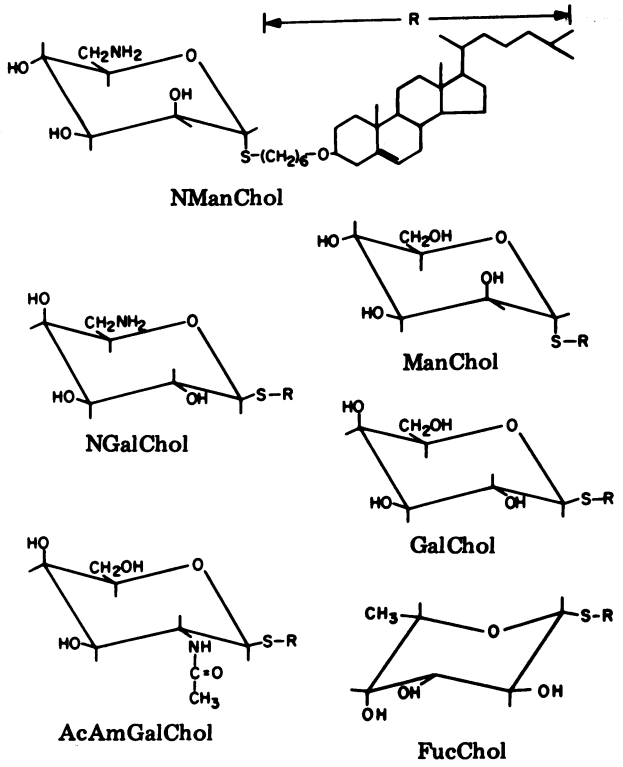

FIG. 1. Chemical structures for the derivatives of cholesterol used in these studies.

loaded with $^{111}In^{3+}$ under conditions described (5, 7) by utilizing A23187 to facilitate the transport of the $^{111}In^{3+}$ to the chelator, $N(AcOH)_3$, inside the vesicles.

Studies *in Vivo*. Vesicles containing $^{111}In^{3+}$ were administered to Swiss–Webster mice (18–22 g) by intravenous (tail vein) or subcutaneous injection (near midline of the back at the level of the scapulae). The amount of $^{111}In^{3+}$ administered ranged between 10 and 160 μCi per mouse depending on the type of experiment (5). The tissue distribution of injected radioactivity was determined by assaying all portions of the mouse in a well-type γ-ray spectrometer. All recoveries were corrected to account for decay of the $^{111}In^{3+}$ ($t_{1/2}$ = 2.8 days). Typically, 4–12 mice were used for each group of time points.

To determine the residual blood content in various tissues, the tissue distribution of $^{111}In^{3+}$ was measured at 8 min after intravenous injection of radiolabeled $Ste_2PtdCho/Chol$ vesicles (Table 1). Assuming that blood comprises 7.3% of the total weight of the animals, we found that 89.6 ± 14.1% of the injected radioactivity was in the blood. Thus, at 8 min, the vesicles were still principally in the bloodstream and the distribution of activity among the various tissues given in Table 1 represents the blood content of the various tissues. The values in Table 1 are in good agreement with previously reported organ blood content levels (11). All tissue distributions reported at longer times are corrected for the activity due to residual blood content. For studies involving both intravenous and subcutaneous administration, the distributions are given as a percentage of the total recovered $^{111}In^{3+}$ because some loss may occur from the injection site, and errors can also occur in the measurement of the injected volumes. In all cases, blood was assumed to comprise 7.3% of the total weight of the animal.

Table 1. Distribution of $^{111}In^{3+}$ 8 min after intravenous injection of radiolabeled $Ste_2PtdCho/Chol$ vesicles

Tissue	%	Tissue	%
Blood*	38.9 ± 4.4	Small intestine	2.5 ± 0.4
Heart	1.4 ± 0.5	Large intestine	0.9 ± 0.2
Lung	1.3 ± 0.2	Brain	0.7 ± 0.1
Liver	10.8 ± 2.5	Abdominal tissue	8.5 ± 1.6
Spleen	1.0 ± 0.2	Chest tissue	10.3 ± 1.2
Kidney	1.8 ± 0.2	Extremities	4.7 ± 0.8
Stomach	0.5 ± 0.1	Skull	11.0 ± 2.2
		Skin	5.9 ± 1.2

Reported as the mean (±SD) percentage of recovered radioactivity found in each tissue. The total recovery of injected radioactivity was 102.1 ± 2.7%.

* Amount of radioactivity in recovered blood and tissue wash fluid.

Autoradiograms of the skin were made in the following manner. The pelt was carefully stretched over a flat surface, internal side facing up. Al foil (25 μm) was placed over the pelt to protect the film (Kodak medical x-ray) which was sandwiched between the foil and a sheet containing activated ZnS phosphor. Exposure time was approximately 15 min.

Cytological characterization of nodules was based on microscopic examination. The tissue specimens were prepared for conventional microscopy by first embedding the sample in paraffin; 4-μm sections were cut, stained, for 5 min in Harris hematoxylin/eosin reagent, and washed with water.

RESULTS

Intravenous Injection. The $Ste_2PtdCho/Chol/NManChol$ vesicles showed substantially greater stability after intravenous administraiqn than did the other vesicle systems tested (Fig. 2). The corresponding tissue distributions also indicate an anomalous behavior for these vesicles (Table 2). In particular, $Ste_2PtdCho/Chol/NManChol$ vesicles cleared rapidly from the bloodstream and showed early retention in lung tissue. At longer times (i.e., >3 hr), the levels of $^{111}In^{3+}$ in the liver and spleen were significantly higher for the aminomannose-bearing vesicles than for other systems examined. PAC measurements on tissue isolated 3 hr after intravenous injection of $Ste_2PtdCho/Chol/NManChol$ vesicles showed that 97% of the vesicles in the lungs, 97% of those in the liver, and 83% of those in the spleen were intact. Similar studies with $Ste_2PtdCho/Chol$ vesicles showed only 56% of those in the liver and 80% of those in the spleen to be intact at 3 hr. At 24 hr, PAC examination of liver showed that 55% of the vesicles in that organ were still intact for the $Ste_2PtdCho/Chol/NManChol$ system compared with only 18% for the $Ste_2PtdCho/Chol$ system. A positive surface charge alone does not produce increased stability because at 12 hr with the $Ste_2PtdCho/Chol/NSte$ system only 16% of the $^{111}In^{3+}$ in the liver was in intact vesicles and no intact vesicles were found in the spleen. The substantially greater stability of

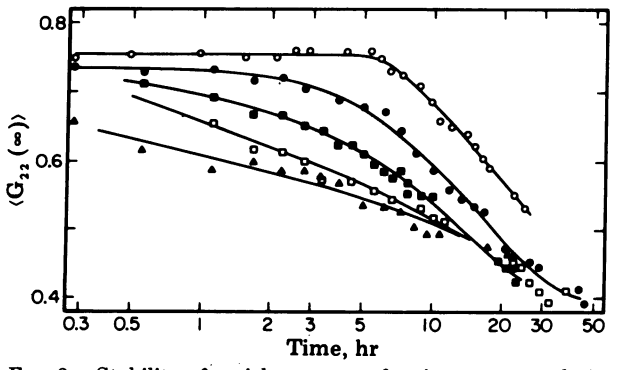

FIG. 2. Stability of vesicle systems after intravenous administration in live mice as measured by PAC. Each set of points is the average from two mice. ●, $Ste_2PtdCho/Chol$; ▲, $Ste_2PtdCho/Chol$-Cet_2P; ■, $Ste_2PtdCho/Chol/GalChol$; □, $Ste_2PtdCho/Chol/NSte$; ○, $Ste_2PtdCho/Chol/NManChol$.

Table 2. Tissue distribution (%) of $^{111}In^{3+}$ after intravenous injection of vesicles

Tissue	$Ste_2PtdCho/Chol$			$Ste_2PtdCho/Chol/Cet_2P$		$Ste_2PtdCho/Chol/NSte$		$Ste_2PtdCho/Chol/GalChol$		$Ste_2PtdCho/Chol/NManChol$		
	1 hr	3 hr	24 hr	3 hr	24 hr	3 hr	24 hr	3 hr	24 hr	1 hr	3 hr	24 hr
Blood	85.5 ±0.6	54.4 ±9.3	6.0 ±2.9	38.4 ±4.9	6.5 ±2.1	28.1 ±7.1	5.9 ±1.7	38.2 ±6.5	2.0 ±1.8	2.1 ±0.5	1.0 ±0.2	0.3 ±0.1
Heart	0.1	0.4	0.4	0.2	0.4	0.1	0.4	0.1	0.4	0.8	0.1	0.1
Lung	0.7 ±0.3	1.9 ±1.2	1.3 ±1.0	0.8 ±0.2	0.5 ±0.1	1.5 ±0.7	0.5 ±0.1	1.0 ±0.6	0.6 ±0.2	24.0 ±5.2	5.9 ±3.8	1.2 ±0.4
Liver	3.3 ±0.1	14.5 ±2.7	30.4 ±9.9	12.9 ±4.3	20.6 ±3.5	50.6 ±2.9	51.5 ±6.2	13.9 ±1.6	37.2 ±8.8	31.6 ±3.8	66.8 ±8.3	65.8 ±1.0
Spleen	0.6	1.8	4.1	2.8	1.9	3.0	2.3	1.1	2.4	3.5	7.4	8.5
Kidney	1.2	1.9	2.7	2.5	4.3	1.1	1.9	2.1	4.2	4.6	1.8	1.8
Stomach	0.2	0.4	0.9	0.3	1.4	0.3	0.5	0.3	0.7	0.7	0.2	0.2
Small int.	2.5	6.1	10.9	7.2	14.2	3.8	4.8	7.5	10.5	5.0	1.6	1.2
Large int.	0.4	2.1	3.9	3.1	4.4	1.1	1.3	2.5	3.7	1.7	0.8	0.8
Brain	*	0.1	*	0.1	*	*	*	0.1	*	0.2	*	*
Abd. & chest	3.3	7.6	14.6	13.8	17.9	4.9	11.6	13.5	16.4	13.6	6.7	9.9
Extremities	2.1	3.1	8.8	5.8	7.4	2.1	9.1	7.0	7.3	3.2	3.4	5.4
Skull	*	1.8	5.3	3.3	7.3	0.3	3.6	3.1	5.0	3.7	1.8	2.7
Skin	*	3.8	10.7	8.8	13.2	3.1	6.6	9.6	9.7	5.4	2.6	2.2
% recovered:												
Injected dose	99	98	104	98	100	95	96	101	100	102	104	106
Blood	40.8	38.6	41.7	41.9	30.8	24.9	50.8	35.6	25.0	33.3	40.0	44.1

All values were corrected for the radioactivity in tissue blood; blood was assumed to comprise 7.3% of the total weight of the animal. Values for blood, lung, and liver include ± SD.
* Value less than 0.1%.

the aminomannose-bearing vesicles observed in these tissues accounts for the overall increased longevity observed in live animals with this system (Fig. 2).

Subcutaneous Injection. Distributions of radioactivity among various tissues following subcutaneous injection are shown in Table 3 for various different vesicle compositions. For the first 12 hr after subcutaneous injection, the tissue distributions for all vesicle systems examined were similar (Table 3). However, at long times (e.g., >72 hr), some differences in the tissue distributions were apparent. In particular, the aminomannose-bearing vesicles showed a higher level of $^{111}In^{3+}$ in the skin than observed with the other vesicle systems, whereas the fraction retained in the liver appeared to increase for the non-aminomannose systems. It is of interest that the aminomannose vesicle system which retained a high fraction of activity in the skin at long times is also the system shown previously (8) to have an extremely long half-time for vesicle destruction (i.e., 600 hr) after subcutaneous injection.

Within 1 hr after subcutaneous injection of vesicles bearing the aminosugar derivatives of cholesterol, a moist appearing, blister-like structure could be seen with the unaided eye. The swelling has been observed up to 8 hr after injection. With

Table 3. Tissue distribution (%) of recovered $^{111}In^{3+}$ after subcutaneous injection of vesicles

Tissue	Ste_2-PtdCho/Chol			Ste_2-PtdCho/Chol/Cet_2P				Ste_2-PtdCho/Chol/NSte			Ste_2-PtdCho/Chol/GalChol			Ste_2-PtdCho/Chol/NManChol			
	0–24 hr	24–72 hr	>72 hr	0–12 hr	12–24 hr	24–72 hr	>72 hr	0–24 hr	24–72 hr	>72 hr	0–24 hr	24–72 hr	>72 hr	0–24 hr	24–72 hr	72–240 hr	>240 hr
Blood	1.0	0.2	0.2	1.5	1.7	0.3	0.1	0.5	0.4	0.5	0.8	0.2	0.1	2.1	0.2	0.09	0.2
Heart	0.03	0.05	0.06	0.03	0.07	0.06	0.1	*	0.02	0.06	0.03	0.03	0.04	0.05	0.02	0.04	0.04
Lung	0.1	0.2	0.2	0.1	0.3	0.1	0.4	0.02	0.05	0.1	0.04	0.04	0.06	0.08	0.03	0.06	0.06
Liver	2.4	3.5	8.7	1.8	7.7	7.1	11.9	0.3	1.6	4.0	2.2	4.5	6.1	1.3	2.1	2.8	2.4
Spleen	0.1	0.2	0.6	0.3	0.9	0.6	1.5	0.1	0.1	0.3	0.07	0.2	0.2	0.1	0.2	0.1	0.1
Kidney	0.2	0.6	0.8	0.3	0.7	0.8	0.9	0.2	0.8	1.2	0.3	0.5	0.6	0.5	0.6	0.6	0.6
Stomach	0.1	0.1	0.1	1.2	0.2	0.2	0.2	0.9	0.1	0.2	0.06	0.09	0.1	0.2	0.09	0.2	0.08
Small int.	0.8	1.0	1.5	1.2	2.6	2.2	2.5	0.5	0.9	1.1	0.7	1.1	1.0	1.2	0.7	0.3	0.5
Large int.	0.6	0.4	0.7	0.5	1.1	0.9	1.2	0.8	0.5	0.9	0.5	0.5	0.4	0.8	0.5	0.2	0.3
Brain	*	*	*	*	0.02	*	0.02	*	*	0.02	*	*	*	*	0.02	0.03	0.02
Abd. & chest	17.5	18.8	18.3	16.7	20.6	18.7	21.9	18.1	19.4	19.2	19.9	20.8	22.3	15.2	13.6	12.6	16.5
Extremities	0.5	1.6	1.6	3.3	2.4	4.6	4.4	0.5	0.8	1.2	0.7	1.7	1.5	1.1	0.8	1.0	1.1
Skull	0.5	0.9	1.0	0.5	1.8	1.5	1.9	0.3	0.7	1.4	0.7	1.6	1.6	0.6	0.8	1.0	0.9
Skin†	76.2 ±8.3	72.6 ±3.4	66.4 ±4.0	72.6 ±8.7	60.1 ±4.7	63.1 ±6.3	53.0 ±5.6	78.0 ±14.1	74.7 ±11.4	69.8 ±7.2	73.9 ±5.5	68.9 ±3.2	66.0 ±9.2	76.9 ±6.6	80.3 ±15.6	81.1 ±10.0	77.3 ±10.2
% injected dose recovered	97	99	104	96	98	101	95	ND	ND	102	100	102	90	ND	ND	95	99

All values were corrected for the radioactivity in tissue blood. ND, not determined.
* Values less than 0.02%.
† Values for skin include ± SD.

FIG. 3. Autoradiographic evidence for the localization of vesicles. An autoradiogram of the skin was prepared and the portion coinciding with the bleb is shown here.

multilamellar vesicles bearing the aminomannose derivative, the localized swelling persisted up to 22 hr after subcutaneous administration.

The blebs coincided with the location of the $^{111}In^{3+}$ (Fig. 3). The pattern observed in the autoradiogram shows that the bleb does not represent intact migration of the injection bolus. The radioactivity appeared confined within a fibrous structure. The bleb was examined on 4-μm-thick tissue sections by using a phase-contrast procedure and was found to be comprised of aggregates of polymorphonuclear leukocytes (Fig. 4).

From the specific activity of the skin tissue, it was apparent that the Ste_2PtdCho/Chol/NManChol vesicles were severalfold more concentrated in the skin than were vesicles of other compositions—for example, Ste_2PtdCho/Chol/GalChol vesicles. Because the PAC results must be corrected for the finite geometry of the radioactive samples analyzed, the observed $\langle G_{22}(\infty)\rangle$ values can be used as an additional means of estimating the concentration of these vesicles. For the aminosugar-bearing vesicles, the $\langle G_{22}(\infty)\rangle$ values on portions of the skin containing radioactivity showed an initial decline not observed with other vesicle systems (Fig. 5). The effective sample volume at these times can be estimated from standard geometric corrections for the PAC spectrometer. For example, reduction of sample size from a sphere of 200 μl to a sphere of 75 μl results in a 25% reduction in the apparent $\langle G_{22}(\infty)\rangle$ value. As indicated in Fig. 5, a 50% reduction in the amount of NManChol derivative in the vesicle bilayer substantially reduced this geometric effect and also reduced the *in vivo* vesicle stability.

FIG. 4. Bleb structure. The blisters are formed of channels between the deep fascia and the muscle layer of subcutaneous tissue containing large numbers of polymorphonuclear leukocytes.

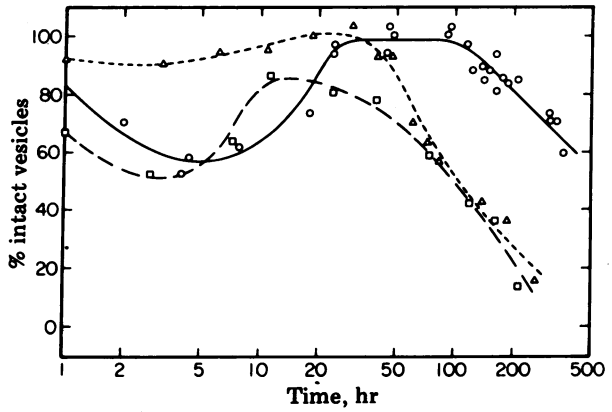

FIG. 5. PAC evidence for the localization of aminosugar-bearing vesicles after subcutaneous injection. ○, Ste_2PtdCho/Chol/NManChol, 2:0.5:0.5 (molar ratio); □, Ste_2PtdCho/Chol/NGalChol, 2:0.5:0.5; △, Ste_2PtdCho/Chol/NManChol, 2:0.75:0.25.

DISCUSSION

Modification of the surface characteristics of lipid vesicles through incorporation into the bilayer of various derivatives of cholesterol has been shown to alter markedly the *in vivo* stability and tissue specificity of the vesicles. Of the derivatives studied, those with a primary amine group at C-6 of the sugar moiety showed the most enhanced stability. When administered subcutaneously, *in vivo* half-times of 100 and 600 hr were found for the aminogalactose and aminomannose systems, respectively, compared to a half-time of 21 hr for the control Ste_2PtdCho/Chol systems (8). This is a much greater enhancement than anticipated from findings with unsubstituted sugar derivatives or with NSte incorporated into the bilayer. The effects observed with the aminosugar derivatives may be attributed to the stereochemical positioning of the amino group at C-6. This amine should be highly exposed on the vesicle surface. The differences in *in vivo* stability between the aminogalactose- and aminomannose-bearing vesicles may arise from two types of stereochemical changes. One of these is a structural difference at the anomeric carbon. The galactose derivatives used here were β isomers; the mannose derivatives were α isomers. The other type of change is epimerizations at C-2 and C-4. With the derivatives available, the relative effects of these two types of changes cannot yet be evaluated.

The population of amine groups on the vesicle surface also is an important factor in vesicle behavior. A 50% reduction in the amount of aminomannose derivative (i.e., Ste_2PtdCho/Chol/NManChol at 2:0.75:0.25) caused a substantial reduction in the extent of localization and a marked decrease in *in vivo* vesicle stability. As reported (8), when the level of aminomannose is lowered still further (i.e., Ste_2PtdCho/Chol/NManChol at 2:0.9:0.1), no bleb formation is observed in the

axillary space. This suggests that a certain concentration of groups on the vesicle surface is required to produce the longevity and tissue specificity observed. Such a dose–response effect is not unique. For example, in studying model systems for cell–cell agglutination, Curatolo *et al.* (12) found that vesicles must contain at least 5 mol % of the glycolipid lactosylceramide to be agglutinated by a plant lectin. At higher glycolipid contents, agglutination increased with increasing glycolipid content.

The anomalous behavior exhibited by vesicles bearing aminosugar derivatives of cholesterol suggests that a particular receptor topography is important in the mechanism leading to transport and destruction of these vesicles. After subcutaneous injections, these vesicles do not remain at the site of injection but are found in blebs in the axillary space. The blebs are filled with aggregates of polymorphonuclear leukocytes. The detailed explanation for these effects must include steps such as the recognition of the aminosugar receptor analogues, the production of a chemotactic factor to attract the leukocytes, the transport of the vesicles along with the leukocytes to the axillary space, and the eventual destruction of the vesicles.

Information on whether similar steps are involved in the processing of aminosugar-bearing vesicles when they are injected intravenously is obtained from tissue distribution data for aminomannose-bearing vesicles. With this vesicle system, a pattern of rapid clearance from the blood with early deposition in the lungs and then subsequent accumulation in liver and spleen is observed. Comparison of these data with patterns observed after intravenous administration of ^{111}In-oxine-labeled leukocytes (13, 14) reveals little similarity. However, our data bear a marked resemblance to tissue distributions observed after administration of ^{111}In-oxine-labeled heat-damaged leukocytes in both rats (13) and rabbits (15). Thus our intravenous results suggest that, after recognition, the aminomannose vesicles could interact with similar cell types, causing these cells to undergo a change (e.g., in surface markers) that leads to these cells being earmarked for destruction. The aminomannose vesicles might remain with the cell, with the vesicles existing intact for extended periods, and hence would exhibit the tissue distribution observed for heat-killed cells.

Our approach of systematically investigating surface groups on lipid vesicles is directed at identifying modifications that will allow the vesicles to be recognized by specific tissues. Various other approaches including use of specific antibodies (16) and receptor-bearing particles (17) have been tried in attempts to achieve targeting. Our experimental results with carbohydrates as phospholipid vesicle surface modifications are consistent with the growing body of information implicating glycolipids as cell surface receptors (2, 12, 18). Our findings indicate that further study of mechanisms of recognition and transport of aminosugar-labeled vesicles *in vivo* and examination of additional carbohydrate derivatives could provide a major advance toward achieving targeting and controlled release of vesicle contents.

We thank Dr. R. L. Teplitz and Susan Clark (City of Hope Medical Center, Duarte, CA) for histological identifications. We also thank Drs. T. Y. Shen and M. M. Ponpipom (Merck, Sharp & Dohme Research Laboratories, Rahway, NJ) for valuable discussion during this work. This investigation was supported by National Institutes of Health Grant GM21111-07, National Science Foundation Grant CHE 79-18401 and a grant from Merck & Co., Inc. This is contribution no. 6194 from the Arthur Amos Noyes Laboratory of Chemical Physics.

1. Pagano, R. E. & Weinstein, J. N. (1978) *Annu. Rev. Biophys. Bioeng.* **7**, 435–468.
2. Hughes, R. C. & Sharon, N. (1978) *Nature (London)* **274**, 637–638.
3. Huang, R. T. (1978) *Nature (London)* **276**, 624–626.
4. Bussian, R. W. & Wriston, J. C., Jr. (1977) *Biochim. Biophys. Acta* **471**, 336–340.
5. Mauk, M. R. & Gamble, R. C. (1979) *Proc. Natl. Acad. Sci. USA* **76**, 765–769.
6. Hwang, K. J. & Mauk, M. R. (1977) *Proc. Natl. Acad. Sci. USA* **74**, 4991–4995.
7. Mauk, M. R. & Gamble, R. C. (1979) *Anal. Biochem.* **94**, 302–307.
8. Mauk, M. R., Gamble, R. C. & Baldeschwieler, J. D. (1980) *Science* **207**, 309–311.
9. Ponpipom, M. M., Bugianesi, R. L. & Shen, T. Y. (1980) *Can. J. Chem.* **58**, 214–220.
10. Lawaczeck, R., Kainosho, M. & Chan, S. I. (1976) *Biochim. Biophys. Acta* **443**, 313–330.
11. McDougall, I. R., Dunnick, J. K., Goris, M. L. & Kriss, J. P. (1975) *J. Nucl. Med.* **16**, 488–491.
12. Curatolo, W., Yau, A. O., Small, D. M. & Sears, B. (1978) *Biochemistry* **17**, 5740–5744.
13. Rannie, G. H., Thakur, M. L. & Ford, W. L. (1977) *Clin. Exp. Immunol.* **29**, 509–514.
14. Lavender, J. P., Goldman, J. M., Arnot, R. N. & Thakur, M. L. (1977) *Br. Med. J.* **2**, 797–799.
15. Thakur, M. L., Coleman, R. E. & Welch, M. J. (1977) *J. Lab. Clin. Med.* **89**, 217–228.
16. Gregoriadis, G. & Neerunjun, D. E. (1975) *Biochem. Biophys. Res. Commun.* **65**, 537–544.
17. Juliano, R. L. & Stamp, D. (1976) *Nature (London)* **261**, 235–238.
18. Critchley, D. R., Ansell, S. & Dilks, S. (1979) *Biochem. Soc. Trans.* **7**, 314–319.